Design of Cosine Modulated Very Selective Suppression Pulses for MR Spectroscopic Imaging at 3T

Joseph A. Osorio,[1,2*] Duan Xu,[2] Charles H. Cunningham,[3] Albert Chen,[2] Adam B. Kerr,[4] John M. Pauly,[4] Daniel B. Vigneron,[1,2] and Sarah J. Nelson[1,2]

The advantages of using a 3 Tesla (T) scanner for MR spectroscopic imaging (MRSI) of brain tissue include improved spectral resolution and increased sensitivity. Very selective saturation (VSS) pulses are important for maximizing selectivity for PRESS MRSI and minimizing chemical shift misregistration by saturating signals from outside the selected region. Although three-dimensional (3D) PRESS MRSI is able to provide excellent quality metabolic data for patients with brain tumors and has been shown to be important for defining tumor burden, the method is currently limited by how much of the anatomic lesion can be covered within a single examination. In this study we designed and implemented cosine modulated VSS pulses that were optimized for 3T MRSI acquisitions. This provided improved coverage and suppression of unwanted lipid signals with a smaller number of pulses. The use of the improved pulse sequence was validated in volunteer studies, and in clinical 3D MRSI exams of brain tumors. Magn Reson Med 61:533–540, 2009. © 2008 Wiley-Liss, Inc.

Key words: very selective suppression; cosine modulation

Point-resolved spectroscopy (PRESS) combined with three-dimensional (3D) phase encoding is commonly used for acquiring clinical magnetic resonance spectroscopic imaging (MRSI) data. This provides metabolic data with excellent quality for patients with brain tumors and has been shown to be important for defining tumor burden (1–5). This method is currently limited by how much of the anatomic lesion can be covered within a single examination. One of the major reasons for this is that the PRESS selection is rectangular, whereas the head is more elliptical in shape. Another complication is the effect of chemical misregistration for the selected volumes of different metabolites. While these issues may be partially addressed by using graphically prescribed outer volume suppression (OVS) pulses to conform the PRESS selected volume to the borders of the brain and to avoid contamination from subcutaneous lipid, the limits on power deposition based upon the estimated specific absorption rate (SAR) restrict the number of such pulses that can be applied at 3 Tesla (T) (6,7).

At lower field strengths, OVS was successful in a clinical setting shown through the use of very selective suppression (VSS) pulse design (7). These pulses can be used with body coil excitation (7), have a relatively large bandwidth compared with previous spatial saturation schemes (8–11) and relatively low radiofrequency (RF) peak power. The high bandwidth minimizes chemical shift errors and produces sharp transition bands that can be used to sharpen the edges of the selected volume. The increased signal to noise ratio (SNR) that is associated with higher field strength and multi-channel phased array coils is becoming more frequently used for clinical applications (12). VSS pulse characteristics therefore become an important limiting factor for minimizing chemical misregistration effects at the edges of the selected region.

The current study presents a cosine modulated VSS (CM-VSS) pulse that was optimized for MRSI at 3T to obtain improved suppression with a smaller number of pulses. PRESS localization was combined with an improved OVS scheme to obtain larger coverage for ^{1}H MR Spectroscopic Imaging (^{1}H MRSI) of the human brain. This was achieved by integrating fixed, cosine-modulated, and graphically defined noncosine modulated, VSS pulses that were optimized for high field strengths (13). The clinical applicability of the CM-VSS pulse scheme was then evaluated in MRSI studies of supratentorial brain regions from various head sizes, shapes, and patients with brain tumors.

METHODS

RF Pulse Design

A nonlinear phase Shinnar-Le Roux (SLR) (14) RF pulse with a time-bandwidth of 18 was designed with the phase optimized to minimize the peak RF power, using methods described previously (15,16). This RF pulse was used as the basis for creating a cosine modulated very selective suppression (VSS) pulse (see Fig. 1a). The low stopband ripple (0.01) and nonlinear phase of the basis RF pulse were designed so that there would be minimal interaction between the dual suppression bands of the cosine modulated pulse. The VSS pulse had a nominal B1 of 0.116 G, a pulse width of 3.0 ms, and a bandwidth that was 5868 Hz. The flip angles of the VSS pulses that were used in this application varied from 91–105°.

Two parallel symmetric suppression bands were produced using a single RF pulse that was modulated directly by a cosine function ($\cos 2\pi f_o t$). The cosine modulated VSS

[1]UCSF/UCB Joint Graduate Group in Bioengineering, San Francisco, California.

[2]Department of Radiology, University of California, San Francisco, California.

[3]Sunnybrook Health Sciences Center for Department of Medical Biophysics, University of Toronto, Toronto, Ontario, Canada.

[4]Department of Electrical Engineering, Stanford University, Stanford, California.

Grant sponsor: National Institutes of Health; Grant number: P50 CA97297; Grant number: RO1 CA111291; Grant sponsor: UC Discovery Grant jointly with GE Healthcare; Grant number: LSIT01-10107; Grant sponsor: National Institute for General Medical Sciences; Grant number: R25 GM56847.

Grant sponsor: This study was presented in part at the 14th Annual Meeting of ISMRM, Seattle, Washington, USA, 2006.

*Correspondence to: Joseph A. Osorio, UCSF Radiology, Box 2532, Byers Hall Building, 1700 4th Street, Suite 303, San Francisco, CA 94158-2532. E-mail: joseph.osorio@radiology.ucsf.edu

Received 18 April 2008; revised 10 July 2008; accepted 7 September 2008.
DOI 10.1002/mrm.21842
Published online 18 December 2008 in Wiley InterScience (www.interscience.wiley.com).

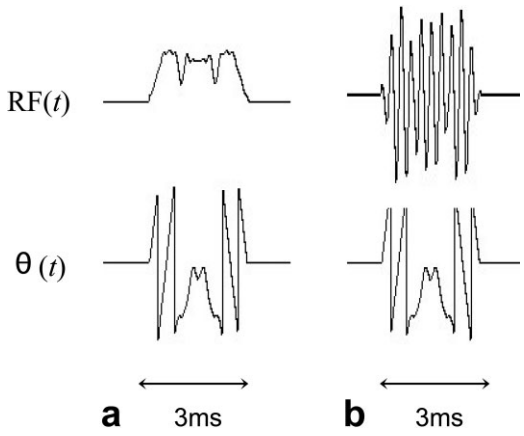

FIG. 1. **a:** RF pulse without cosine modulation. **b:** Cosine modulated VSS pulse.

(CM-VSS) pulse was generated on the MR scanner in real time and produced two suppression bands of equal thickness that were spatially located, and displaced, using the desired volume edge prescription using:

$$FT(\cos\ 2\pi f_o t) = \frac{\delta(f - f_o) + \delta(f + f_o)}{2} \qquad [1]$$

where f is the frequency relative to the center of the acquisition volume, and $\pm\ f_o$ is determined from the desired suppression band separation. This separation was computed as the difference from the center of the acquisition volume to the center of the suppression band. The RF pulse waveforms before (a) and after (b) cosine modulation are shown in Figure 1.

The excitation of the cosine modulated pulse was optimized to generate similar suppression as a single VSS pulse while maintaining an adequate power level. This was accomplished by doubling the VSS pulse flip angle to achieve the desired suppression. The CM-VSS pulse flip angles ranged between 182–193°. The duration of the CM-VSS pulse remained the same as a conventional VSS pulse with duration 3 ms.

Crusher gradients were used to eliminate any residual transverse components of magnetization following each VSS pulse, each with a duration of 1 ms. Conventional suppression pulse schemes that generated one suppression band for each VSS pulse use an equal number of crusher gradients as VSS pulses (7). The CM-VSS pulse scheme required only one crusher gradient for every pair of suppression bands that were generated from a single cosine modulated pulse.

The phased modulated low peak power characteristic of the CM-VSS pulse allowed for 12 fixed-suppression bands in addition to the 6 graphically prescribed bands for a total of 18 suppression bands. The pulse sequence used with this suppression pulse scheme is shown in Figure 2. Eight of the 12 fixed cosine modulated suppression bands were used to generate an octagonal selection region in axial slices. The six additional graphically prescribed bands were also used to generate elliptical volume selectivity in the axial plane that specifically conformed the selected region to the shape of the individual head. The remaining four cosine modulated suppression bands were implemented for the superior and inferior sides of the volume selection.

Data Acquisition

The CM-VSS pulse scheme was tested in phantom experiments, normal volunteers, and patients with brain tumors using a PRESS pulse sequence on a GE 3T MR scanner. Signal was received using an eight-channel phased array head coil, with body coil excitation. Chemical shift-selective saturation (CHESS) pulses were used for water suppression. The total acquisition time was 4.5 minutes (TR/TE = 1100/144 ms) for a single slice of MRSI data. These acquisitions used spectral arrays of 16 × 16 × 1 with full *k*-space sampling and fields of view corresponding to a nominal isotropic spatial resolution of 1 cc. Uniformity of the desired range of chemical frequencies was achieved by prescribing a PRESS box that was larger than the region of interest (overpress), and using CM-VSS pulses to suppress signals arising from beyond the region of interest. At 3T, an overpress factor of 1.2 has been shown to significantly improve uniformity and selectivity of MRSI (13). Data were reconstructed using processing software that was customized for the analysis of MRSI studies (17).

The number of slices being considered varied depending on the desired coverage. On average, there were five or six slices acquired. For tumor patients, each slice was individually prescribed to maximize coverage to include maximal tumor coverage, and maximal coverage of surrounding normal tissue. For full coverage, the PRESS box selection included portions of subcutaneous lipid layers, mostly arising in the corners of the box selection. before PRESS box selection, a train of six CM-VSS pulses and six graphically-prescribed conventional VSS pulses all separated by crusher gradients were used to provide outer volume suppression of unwanted signal. The magnetic field homogeneity was optimized using higher order shimming over the volume of interest before each MRSI slice acquisition using the manufacturer-provided routine which is based upon the method described by Kim et al. (18).

Evaluation of Coverage Obtained Using Conventional VSS

To estimate the coverage that is conventionally achieved with VSS pulses, previously scanned patients were analyzed using standard postprocessing methodologies (17). Twenty-eight patients with histologically confirmed tumors of glial origin were evaluated (14 grade II; 14 grade IV). The patients had received varying levels of treatment, including surgical resections, chemotherapy, and/or radiation therapy. Scans were performed on a GE 3T MR scanner with a conventional VSS pulse scheme. Twelve VSS pulses were applied in the 3D MRSI acquisitions using PRESS volume selection, with a TR/TE = 1100/144 ms. CHESS pulses were used for water suppression, and the overpress factor was 1.2. The slice thickness for the MRSI data was 10 mm. The tumor was defined as the area corresponding to the FLAIR abnormality. MRSI coverage was defined by the spatial extent of the PRESS volume selection.

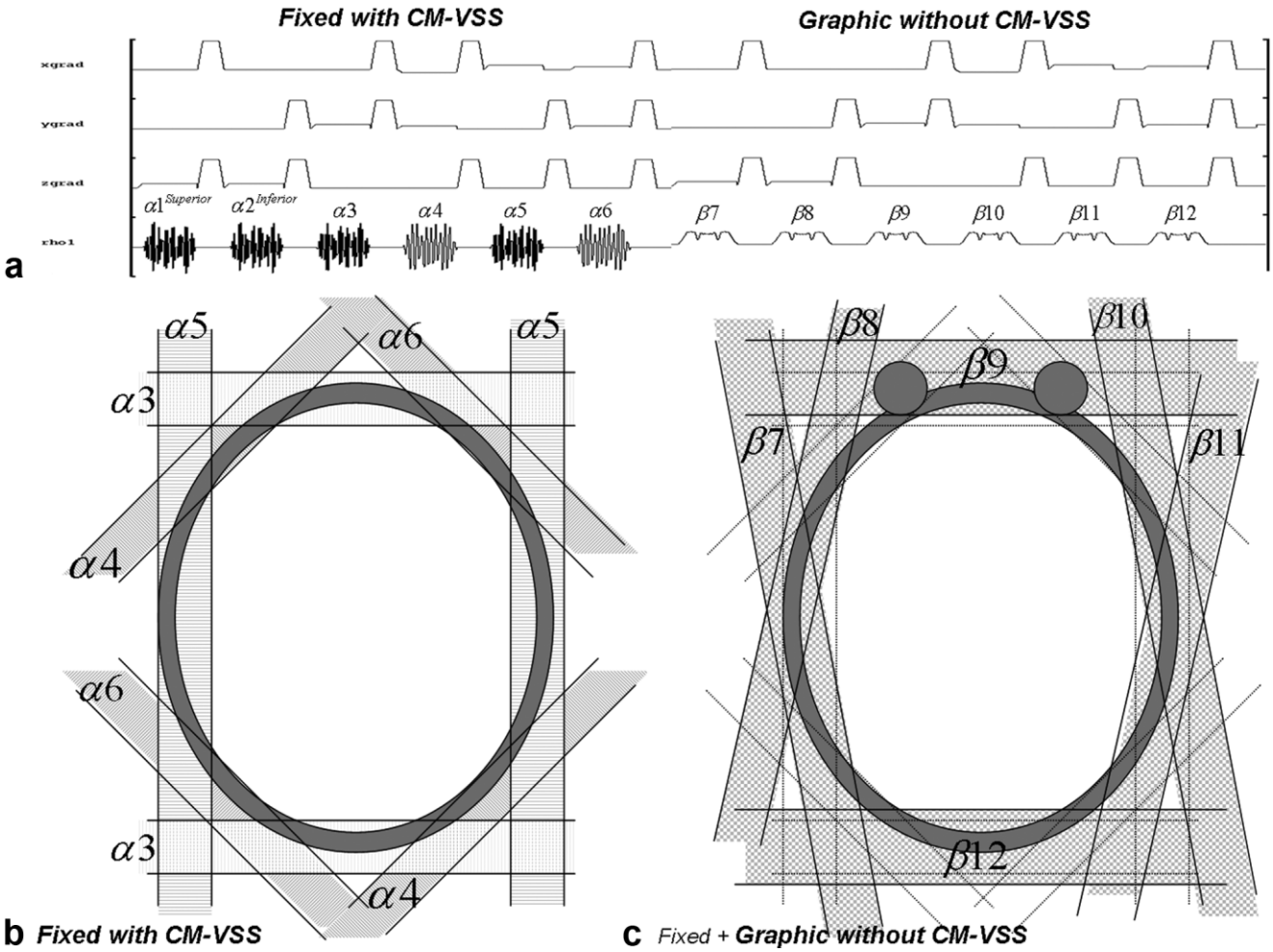

FIG. 2. **a:** The section of the MRSI pulse sequence corresponding to the outer volume suppression scheme. The phased modulated low peak power characteristic of the CM-VSS pulse allowed for 12 fixed-suppression bands in addition to the 6 graphically prescribed bands—a total of 18 suppression bands. **b:** Eight of the 12 fixed cosine modulated suppression bands were used to generate an octagonal selection region in axial slices. **c:** The six additional graphically prescribed bands were also used axially to generate an elliptical volume selectivity that uniquely conformed the selected region to the shape of the individual. The remaining four cosine modulated suppression bands were implemented in the superior and inferior sides of the volume selection.

Application in Brain Tumors

Ten patients were scanned prospectively using both conventional MRSI-VSS methodology and MRSI with the CM-VSS scheme. The same parameters presented above were used to compare coverage, SAR, and to evaluate the data quality between both schemes.

RESULTS

RF Pulse Performance

The performance of the new VSS pulse is demonstrated using spin-echo images that were acquired from a phantom before (a) and after (b) cosine modulation in Figure 3. These data demonstrate that the suppression bands add high spatial selectivity, and there was minimal interaction between the bands (Fig. 3). The performance of the pulse is further demonstrated by the linear profile in Figure 3c, which corresponds to a projection from the center of the image in Figure 3b. Suppression bands were tailored to obtain an ROI representative of an octagon shown in Figure 3d. Two symmetric saturation bands were generated at distances down to 2 mm apart with no interaction between the bands. In the phantoms, the efficiency with which the VSS pulse saturated water was 98%.

The time taken to play out the total number of suppression bands using the modified CM-VSS scheme was less than if the same number of suppression bands were generated using a conventional pulse scheme. This improved water suppression by 17%. In addition, time was conserved further from the additional crusher gradients and the ramp time from the spatial selective gradient. The time saved for each crusher gradient and its respective gradient ramp time was 1.7 ms. Cosine modulation of the VSS pulse along with the phased modulated low peak power characteristic allowed for 18 saturation bands to be implemented in human subjects while still keeping the power deposition under the FDA-approved specific absorption rate (SAR) limit. The current CM-VSS pulse scheme duration

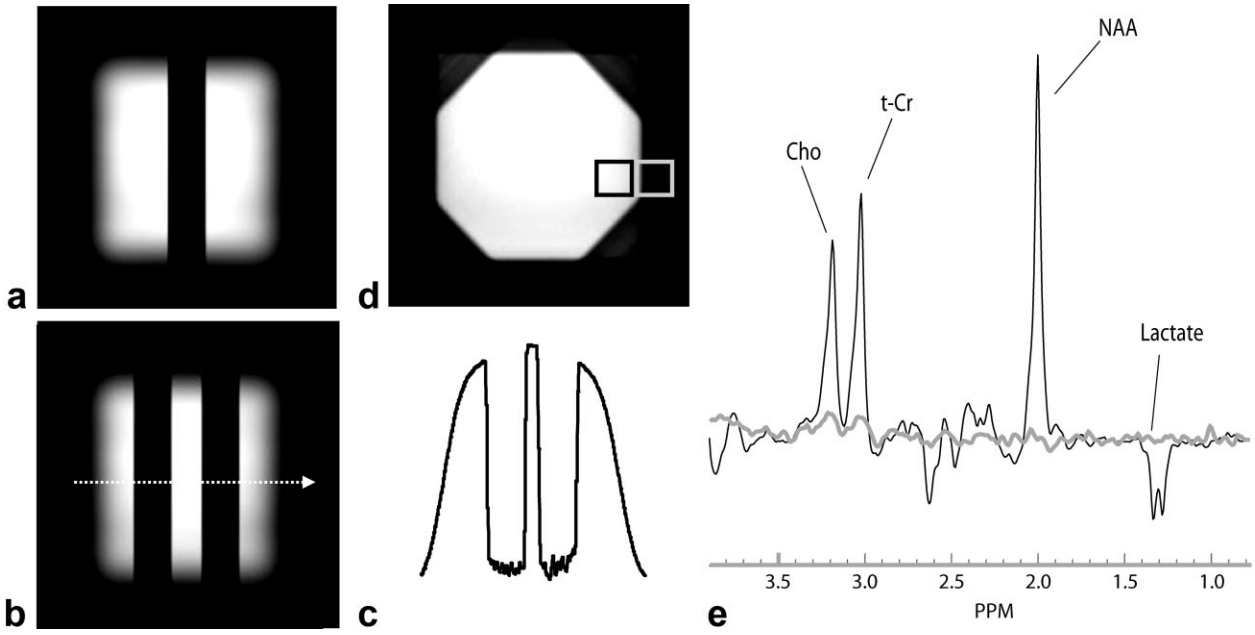

FIG. 3. Demonstration of the functionality of the pulse. **a:** One single band VSS pulse. **b:** One dual-band cosine modulated VSS pulse shown as two symmetric bands. **c:** A linear intensity profile generated from Figure 1b. **d:** Four dual-band cosine modulated VSS pulses making an octagon shaped volume selection. **e:** Two spectra demonstrating the performance at the margins of the selected volume in Figure 1d.

was 56.4 ms producing 18 suppression bands, where conventional non–CM-VSS scheme would have duration of 84.6 ms to generate the same number of suppression bands. Practical implementation of the conventional VSS pulse scheme allowed a maximum of 12 VSS pulses at 3T, limiting the number of suppression bands to 12 with a total duration of 56.4 ms. The current outer volume suppression pulse scheme not only retained the total duration of pulses to 56.4 ms to maintain adequate water suppression, but it additionally provided six extra suppression bands. Table 1 lists the pulse parameters for the various outer volume suppression pulse schemes. Note the use of the CM-VSS scheme allows for a greater number of suppression bands in a shorter duration. The time saved was 28.2 ms when reducing the number of crusher gradients, while using the CM-VSS pulse scheme. This reduced the duration of the outer volume suppression scheme by a third, as shown in Table 1. If the duration of the outer volume suppression scheme were unchanged, the CM-VSS pulse scheme would achieve an additional six saturation bands.

Application in Normal Brain MRSI

The data in Figure 4 show the feasibility of performing an MRSI scan on a volunteer with the PRESS volume conformed to an octagonal-shaped axial selection region. The high spatial selectivity of the suppression bands is demonstrated in the edge transitions of the box image in Figure 4b. Figure 4c shows a spectral array from the normal volunteer with suppression of unwanted signal from outside the volume selection. The efficiency of saturation of water from the CM-VSS pulse was 93% in volunteers.

Increased spatial coverage was achieved in volunteers from MRSI data using the CM-VSS pulse scheme. The metabolite maps in Figure 4d demonstrate MRSI with high spatial selectivity of the suppression bands from multiple acquired slices. Conventional volume selection at 3T for the volunteer scans was on average limited to 67.5 cc for a single slice of MRSI data using 3D acquisitions with 12 VSS pulses. The mean volume selection in volunteers for a single slice acquired with the CM-VSS pulse scheme was 102.8 cc, demonstrating a 1.5 increase in coverage. The irregular selection was conformed to the shape of the head as shown by the NAA map which is overlaid on the MR image from a normal volunteer in Figure 4d.

The data shown in Figure 5 demonstrate the improved lipid suppression throughout the acquired MRSI volume using the CM-VSS scheme when compared with conventional outer volume suppression pulse schemes. The lipid metabolite map overlay shows the most improved lipid

Table 1
Comparison of CM-VSS Pulse Scheme and Conventional VSS: Pulses, Timing, SNR, and SAR

	RF pulses		Crusher gradients	Sat bands	Selection shape	Duration (ms)	Signal-to-noise		SAR (W/kg)
	CM-VSS	VSS					Choline	NAA	
HCM-VSS	6	6	12	18	Octagon	56.4	15.1	26.0	1.4
VSS	0	18	18	18	Octagon	84.6	—	—	—
VSS[a]	0	12	12	12	Rectangle	56.4	13.5	25.9	1.2

[a]PRESS MRSI with conventional outer volume suppression scheme at 3T.

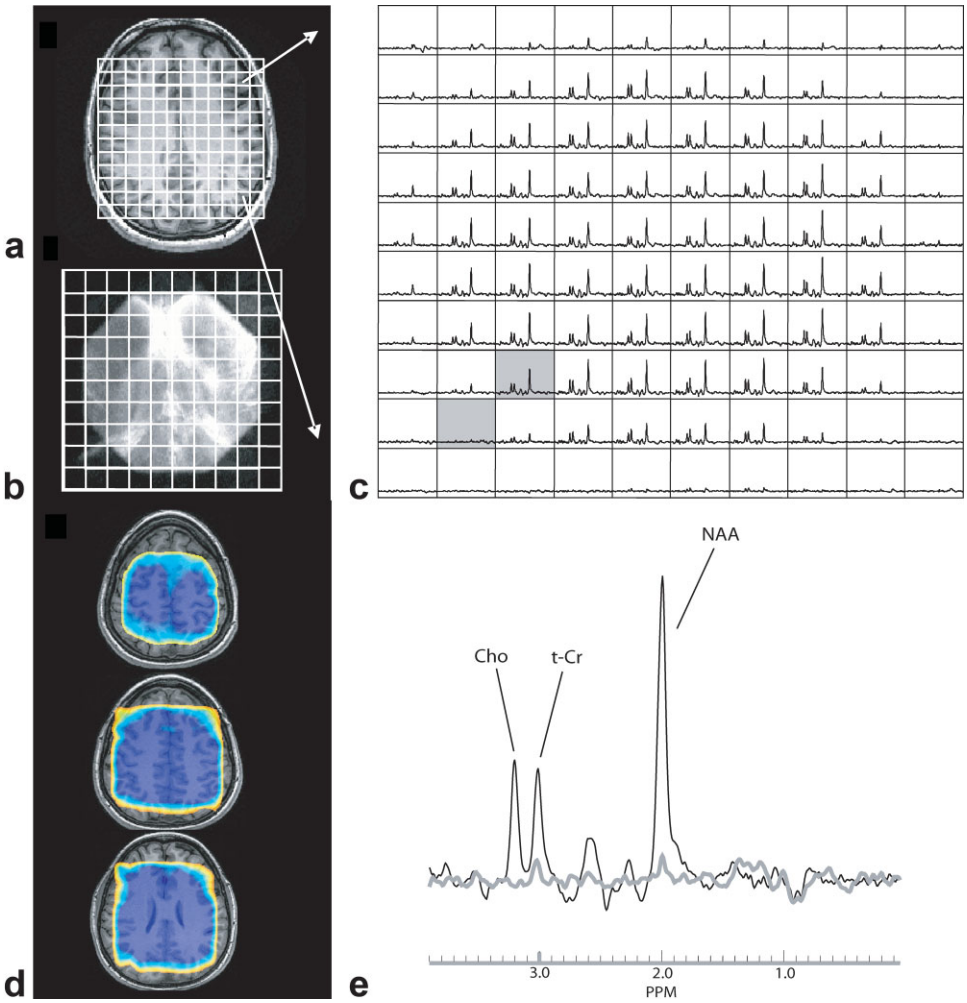

FIG. 4. In vivo volunteer data with four CM-VSS pulses performing eight saturation bands into an octagon shaped volume selection. **a:** T1 SPGR with overlay of MRSI. **b:** MRS selection volume demonstrating the irregular contour. **c:** Full MRSI array demonstrating high quality spectra with desired contour selection. **d:** Normal volunteer multislice example that used cosine modulated PRESS MRSI; color map of NAA peak height is shown overlaid on the T1-weighted images. **e:** Enlarged spectra from regions shaded in gray in Figure 4c.

suppression when using fixed CM-VSS and graphically prescribed VSS pulses—total of 12 RF pulses for OVS. The quality of the MRSI data was analyzed and compared with the conventional MRSI sequence. Signal-to-noise calculations are shown in Table 1 demonstrating comparable data quality to conventional MRSI.

Retrospective MRSI Coverage Analysis in Patient Data

The scans from 28 patients were retrospectively investigated for PRESS MRSI tumor coverage using conventional VSS pulses. These patients had a mean tumor volume of 80 cc that was defined by the FLAIR hyperintensity. Grade II glioma patients had 61% of the tumor included within the MRSI volume, while Grade IV patients had 66% included within the MRSI volume. Nineteen of the 28 patients had tumor sizes smaller than 80 cc and only 68% of these tumors were covered by MRSI. Nine of the 28 patients had large tumors ranging from 80 cc to 167 cc and only 53% of these larger-sized tumors were covered by conventional MRSI. Over the entire group of 28 patients, the MRSI acquisitions had a mean coverage of 63% of the abnormal region.

Application of CM-VSS Pulses to Patients With Brain Tumors

Table 2 shows slice-by-slice coverage comparison in three patients who were studied prospectively using the CM-VSS scheme, with the mean volume of brain tissue covered in patients being 120 cc per MRSI slice. When the number of slices was consistent, there was a 1.9 times improvement in coverage in 10 patients using the CM-VSS scheme, over conventional MRSI. Figure 6 demonstrates a comparison of the PRESS MRSI selected volume using both OVS methods, conventional and optimized CM-VSS respectively. Figure 6c is the FLAIR image of a patient with a brain tumor, with superimposed volume selection regions (cosine modulated VSS and conventional). Figure 6e is a spectrum showing abnormal metabolite ratios from a region that was not able to be included within the limited coverage of the conventional OVS scheme.

Graphically prescribed bands were an important facet of the current implementation of the CM-VSS pulse scheme. The purpose of the graphic suppression bands was twofold, they were used to tailor the outer volume suppression to different head shapes and sizes, and they were critical in situations where additional suppression bands were needed for residual magnetization from excited lipid signal. It was often the case that peri-cranial lipid was excited when the volume prescriptions were increased to reach the extent of the brain tissue. In situations where lipid regions were excited, more than one suppression band was desirable to reduce the consequence of lipid contamination. Excited lipid regions would receive two suppression

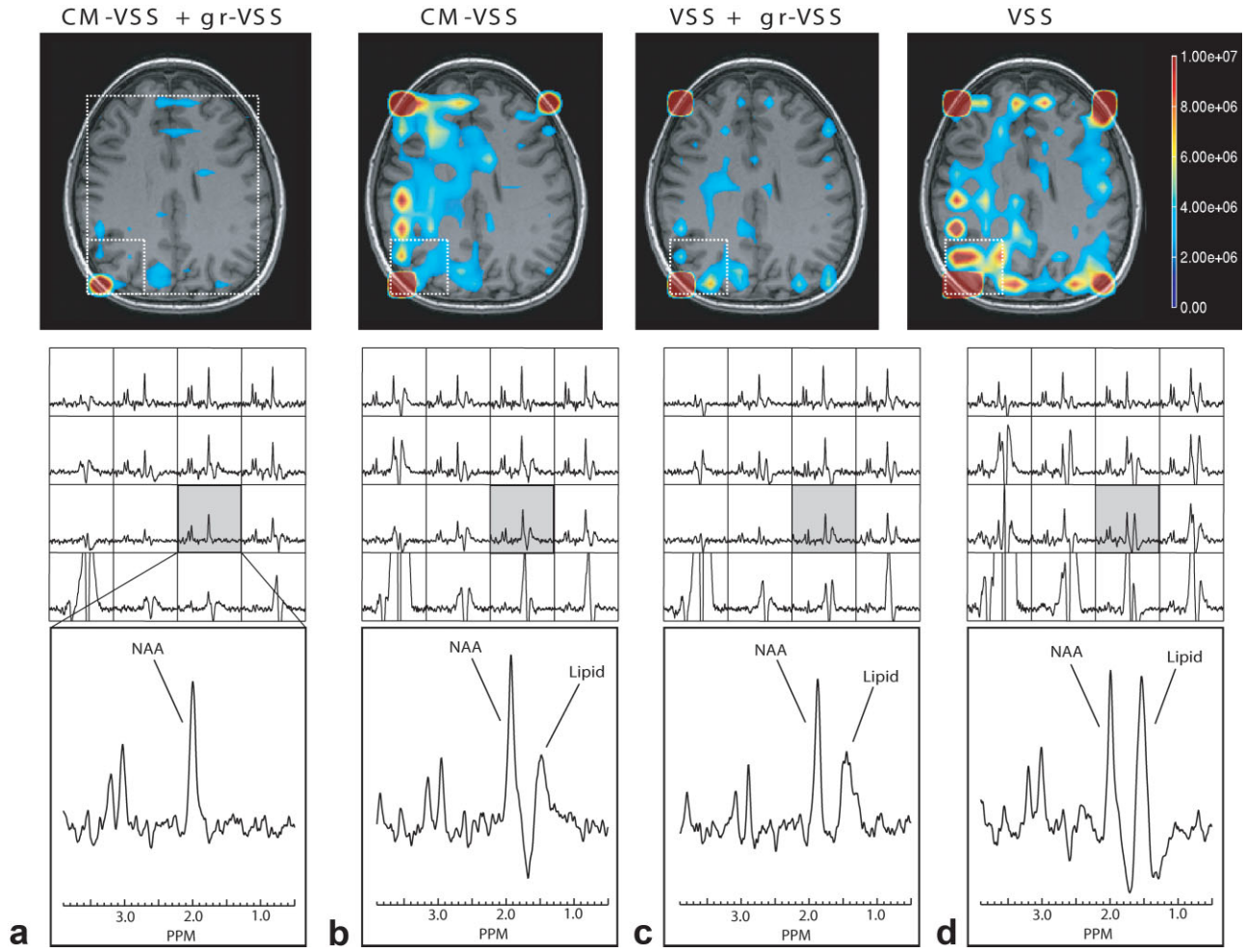

FIG. 5. MRSI data acquired with both the CM-VSS scheme and conventional outer volume suppression scheme. The large box selection on the T_1 weighted images denotes the region excited by RF pulses in the PRESS sequence. The smaller box shows the voxel locations corresponding to the spectra below. Overlay of lipid metabolite map is shown for corresponding T_1 images. **a:** Spectra acquired using fixed CM-VSS pulses and graphic non–CM-VSS pulses—total of 12 RF pulses. **b:** Spectra acquired with only fixed CM-VSS pulses—total of 6 RF pulses. **c:** Spectra acquired using conventional VSS pulses for fixed and graphic prescription—total of 12 RF pulses. **d:** Spectra acquired using VSS pulses for fixed prescription—total of 6 RF pulses.

bands, one from the graphic prescription, and the other from the oblique CM-VSS pulse.

DISCUSSION

RF Pulse Performance

When moving to higher field strength scanners, it is more likely that MRSI acquisitions can exceed the limitation on the amount of RF power that can be deposited. This has had an impact upon the number of OVS pulses that could be used for MRSI studies. Although Tran et. al was successful at introducing an effective OVS pulse that was high spatially selective for PRESS MRSI, the pulse scheme used was optimized for 1.5T scanners (7). The CM-VSS pulse and OVS scheme that is proposed in this study not only takes advantage of the previous improvements introduced

Table 2
MRSI Coverage Comparison in Three Patients [A-C]: Units Are Numbers of Voxels with 10-mm Isotropic Resolution

Slice no.	Conventional [A]	CM-VSS [A]	CM-VSS [B]	CM-VSS [C]
1–(superior)	64	—	90	80
2	64	—	110	120
3	64	132	132	130
4	64	132	132	132
5	—	—	132	132
6–(inferior)	—	—	132	—
Average/slice	64	132	121	119
Total coverage	256	264	728	594

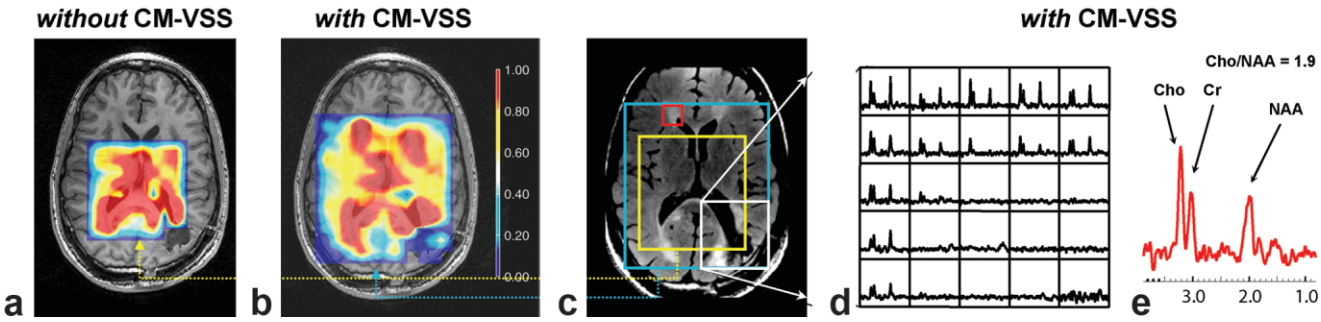

FIG. 6. Brain tumor patient with ^{1}H MRSI using both cosine modulated VSS pulse scheme and conventional. **a,b:** T1-weighted image with Cho-to-NAA overlay from conventional MRSI selection (a), and from MRSI using cosine modulated VSS scheme (b). **c:** FLAIR image with selected regions from (a) and (b). **d:** Example array of spectra shown from selection using (b) cosine modulated VSS scheme. **e:** Spectrum characteristic of abnormal metabolism from voxel outside of conventional coverage.

by the VSS pulse, but also improves coverage and optimizes the outer volume suppression for higher field strength scanners.

Applications in Single Slice and 3D MRSI

This study demonstrated improved results when implementing CM-VSS pulses in a single-slice MRSI acquisition sequence. Although the sequence was designed for maximum 2D coverage, it is not limited to single-slice acquisitions and could be used to acquire 3D-MRSI data with comparable quality, improved outer volume suppression of unwanted signals, and significantly larger coverage over conventional methods. The octagon selection was designed to maximize coverage in the axial dimension, allowing each slice to be adjusted for various head shapes and sizes with varying geometric constraints. The single-slice scheme proposed generates different amounts of coverage for each slice within a given exam and allows for shimming to be adjusted between acquisitions. This is a benefit in regions near the sinuses, or close to surgical cavities where susceptibility effects may otherwise result in signal drop-outs. The trade-off with the use of multiple single slice acquisitions comes at the cost of the time needed to set up additional graphic prescriptions, and lower SNR relative to the comparable 3D scheme.

The single-slice data in this study were acquired at full sampling of *k*-space so that the intrinsic data SNR was comparable to the current standard for 3D MRSI data that are acquired with the same acquisition time. Maximal coverage for a 3D data acquisition in the axial plane is limited by the slice that has the smallest volume of brain parenchyma. This is typically the most superior or the most inferior slice. Although the axial coverage for the intermediate slices would be less using the CM-VSS pulse scheme with 3D rather than multiple 2D volume selections, the data quality would still be better than using conventional OVS schemes with 3D selection because of the improved suppression of unwanted signals from subcutaneous lipid.

Comparison to Alternative OVS Methods

The OVS methods used in our studies perform at high bandwidths and therefore achieve excellent high spatial selectivity. This is important for cases where a larger excitation volume is applied to eliminate chemical shift artifacts within the region of interest and for situations where the selected volume would otherwise contain signal from regions with limited water or lipid suppression. The methods presented also describe pulses that achieve B1 and T1 insensitivity, while still maintaining adequate SNR.

An approach using spin-echo MRSI outer-volume suppression (SELOVS) was recently successfully applied at 3T to significantly enhance brain-MRSI localization, but this required long computational times for the algorithm implementation (19). In standard clinical settings there are significant variations in head shapes and sizes that might limit the usefulness of this technique in its current form. Another factor to be considered is that SELOVS was limited to single-slice acquisitions, and it was expected to exceed SAR in PRESS MRSI applications.

Further Applications

The CM-VSS pulses designed can be useful not only for applications in the brain, but to many other situations that are limited because of lack of suppression of unwanted signals from outside the volume of interest. CM-VSS MRSI is expected to be particularly valuable in prostate and liver, where an octagon-shaped volume acquisition is often desired. The use of higher field strength scanners is also a benefit for SENSE and GRAPPA techniques, which can be used to improve acquisition times in MRSI. The use of CM-VSS in conjunction with these approaches may provide improved suppression of unwanted signals over the conventional methodology and allow these parallel imaging techniques to be used in a more routine setting.

CONCLUSIONS

Improved outer volume suppression pulses for PRESS MRSI were designed and implemented on a 3T MR scanner. The cosine modulated VSS pulses schemes used in this study allowed SAR limits to be satisfied while increasing coverage for high-field MRSI. The quality of the data and efficiency of lipid suppression were demonstrated in both normal volunteers and patients with brain tumors.

The CM-VSS pulse scheme provided a simple, reliable and practical approach for increasing coverage and improving outer volume suppression of unwanted signals for clinical MRSI examinations.

REFERENCES

1. Fulham MJ, Bizzi A, Dietz MJ, Shih HH, Raman R, Sobering GS, Frank JA, Dwyer AJ, Alger JR, Di Chiro G. Mapping of brain tumor metabolites with proton MR spectroscopic imaging: clinical relevance. Radiology 1992;185:675–686.
2. Nelson SJ, Graves E, Pirzkall A, Li X, Antiniw Chan A, Vigneron DB, McKnight TR. In vivo molecular imaging for planning radiation therapy of gliomas: an application of 1H MRSI. J Magn Reson Imaging 2002;16: 464–476.
3. Preul MC, Caramanos Z, Collins DL, Villemure JG, Leblanc R, Olivier A, Pokrupa R, Arnold DL. Accurate, noninvasive diagnosis of human brain tumors by using proton magnetic resonance spectroscopy. Nat Med 1996;2:323–325.
4. Preul MC, Caramanos Z, Leblanc R, Villemure JG, Arnold DL. Using pattern analysis of in vivo proton MRSI data to improve the diagnosis and surgical management of patients with brain tumors. NMR Biomed 1998;11:192–200.
5. Dowling C, Bollen AW, Noworolski SM, McDermott MW, Barbaro NM, Day MR, Henry RG, Chang SM, Dillon WP, Nelson SJ, Vigneron DB. Preoperative proton MR spectroscopic imaging of brain tumors: correlation with histopathologic analysis of resection specimens. AJNR Am J Neuroradiol 2001;22:604–612.
6. Le Roux P, Gilles RJ, McKinnon GC, Carlier PG. Optimized outer volume suppression for single-shot fast spin-echo cardiac imaging. J Magn Reson Imaging 1998;8:1022–1032.
7. Tran TK, Vigneron DB, Sailasuta N, Tropp J, Le Roux P, Kurhanewicz J, Nelson S, Hurd R. Very selective suppression pulses for clinical MRSI studies of brain and prostate cancer. Magn Reson Med 2000;43:23–33.
8. Duyn JH, Gillen J, Sobering G, van Zijl PC, Moonen CT. Multisection proton MR spectroscopic imaging of the brain. Radiology 1993;188: 277–282.
9. Posse S, Schuknecht B, Smith ME, van Zijl PC, Herschkowitz N, Moonen CT. Short echo time proton MR spectroscopic imaging. J Comput Assist Tomogr 1993;17:1–14.
10. Shungu DC, Glickson JD. Band-selective spin echoes for in vivo localized 1H NMR spectroscopy. Magn Reson Med 1994;32:277–284.
11. Singh S RB, Henkelman RM. Projection presaturation: a fast and accurate technique for multidimensional spatial localization. J Magn Reson 1990;87:567–583.
12. Osorio JA, Ozturk-Isik E, Xu D, Cha S, Chang S, Berger MS, Vigneron DB, Nelson SJ. 3D 1H MRSI of brain tumors at 3.0 Tesla using an eight-channel phased-array head coil. J Magn Reson Imaging 2007;26: 23–30.
13. Li Y, Osorio JA, Ozturk-Isik E, Chen AP, Xu D, Crane JC, Cha S, Chang S, Berger MS, Vigneron DB, Nelson SJ. Considerations in applying 3D PRESS H-1 brain MRSI with an eight-channel phased-array coil at 3 T. Magn Reson Imaging 2006;24:1295–1302.
14. Pauly J, Le Roux P, Nishimura D, Macovski A. Parameter relations for the Shinnar-Le Roux selective excitation pulse design algorithm NMR imaging. IEEE Trans Med Imaging 1991;10:53–65.
15. Pickup S, Popescu M. Efficient design of pulses with trapezoidal magnitude and linear phase response profiles. Magn Reson Med 1997;38: 137–145.
16. Shinnar M. Reduced power selective excitation radio frequency pulses. Magn Reson Med 1994;32:658–660.
17. Nelson SJ. Analysis of volume MRI and MR spectroscopic imaging data for the evaluation of patients with brain tumors. Magn Reson Med 2001;46:228–239.
18. Kim DH, Adalsteinsson E, Glover GH, Spielman DM. Regularized higher-order in vivo shimming. Magn Reson Med 2002;48:715–722.
19. Henning A, Schar M, Schulte RF, Wilm B, Pruessmann KP, Boesiger P. SELOVS: brain MRSI localization based on highly selective T1- and B1-insensitive outer-volume suppression at 3T. Magn Reson Med 2008;59: 40–51.